Article

Transactions of the Institute of Measurement and Control
34(8) 966–973

DOI: 10.1177/0142331211427489
tim.sagepub.com

Regional dynamical modeling and control of flow problems under unmeasurable and non-constant viscosity

Türker Nazmi Erbil and Coşku Kasnakoğlu

Abstract

In this paper a novel approach to the modeling and control of flow problems is considered. The main extension over existing methods is the ability to handle a local region of interest, and the capability to deal with the fluid viscosity being non-constant and unmeasurable. For the modeling part, first a number of snapshots of the fluid flow process at different viscosity values are obtained by computational fluid dynamics simulations of the Navier–Stokes equations governing the flow. Wavelet transform, thresholding and reconstruction are applied to these snapshots and it is seen that the flow process can be represented with acceptable accuracy using only the approximation coefficients of the wavelet transform. The support of the basis functions are selected to tightly cover the desired region of interest so that the flow dynamics outside the desired region do not affect the model significantly. Subspace system identification methods are used to fit a low-dimensional dynamical system model to the approximation coefficients, which yields a set of linear time invariant models, one for each breakpoint viscosity. A single uncertain model is built to capture all of the models in this set, and a robust controller is designed for this uncertain model using D-K iteration. The technique is illustrated on a sample flow configuration on a square domain where the input affects the system through the boundary conditions.

Keywords:

Regional dynamical modeling, flow control, unmeasurable viscosity, wavelet transform, Navier Stokes equations, robust control

Introduction

Flow problems, in general, investigate the physical behavior of liquids, gases and other materials which deform (i.e. flow) under an applied shear stress. Examples include the flow of water around submarine hulls, the air flow over the wings of aircraft and the flow inside oil pipelines. The concept of flow control is important from a technical point of view due its potential benefits such as fuel savings for vehicles and efficiency improvement for industrial processes (Gad-el Hak 2000; Bewley 2001). Fluid flow dynamics are usually governed by complicated partial differential equations (PDEs; e.g. Navier–Stokes [NS] equations) which are difficult to handle (Acheson 1990; Batchelor 2000). The most common approach for reducing these PDEs to simpler dynamical models is the proper orthogonal decomposition (POD)/input separation (IS)/Galerkin projection (GP) method. In this approach, one first obtains a set of modes called POD modes, which capture a sufficiently large amount of energy from the flow. The effect of the input entering the system is captured through a process called IS, which yields an additional mode called the actuation mode. The expansion of the flow in terms of these modes is substituted into the governing PDEs and the GP step is applied to obtain the reduced order model of the flow process, the states of which are called the time coefficients. Details of the POD/IS/GP methods can be found in Sirovich (1987), Holmes et al. (1996), Camphouse (2005), Efe and Ozbay (2004), and Kasnakoglu et al. (2008). Although these methods yield low-dimensional dynamic models, the models are nonlinear and thus it is very difficult to utilize them for analysis and control design. Another difficulty in these methods is that the POD modes spread out to the entire flow domain, and hence it is not possible to associate a particular time coefficient with a specific spatial region. A final shortcoming is that in the standard flow control approaches the models and controllers are usually built around a single value of the flow parameters, in particular a single value of the fluid viscosity. The viscosity describes a fluid's internal resistance to flow and may be thought of as a measure of fluid friction. Since the viscosity is dependent on various factors (e.g. temperature, pressure), it is desirable to address situations where these factors and hence the viscosity varies with time. It is also difficult to perform efficient and reliable measurements of a fluid's

Department of Electrical and Electronics Engineering, TOBB University of Economics and Technology, Ankara, Turkey

Corresponding author:
Coşku Kasnakoğlu, Department of Electrical and Electronics Engineering, TOBB University of Economics and Technology, Sogutozu Caddesi No. 43, 06530 Ankara, Turkey
Email: kasnakoglu@etu.edu.tr

viscosity in real-time, hence a controller design which does not rely on such an information would be advantageous.

In this paper, a novel procedure for the modeling and control of flow problems is described, where the goal is to eliminate the shortcomings of the standard modeling techniques described above. The modeling part is based on wavelet transform so as to achieve locality, whereas the control part is based on robust control design via D-K iteration. The paper is organized as follows: Section 2 provides background information on wavelet transform and the NS equations, Section 3 outlines the modeling and control approach proposed, Section 4 illustrates the approach on a sample flow problem and Section 5 provides conclusions and future work ideas.

Background information

Wavelet transform

The wavelet transform is one of the most commonly used techniques in signal processing on which a large number of resources and studies are available (Chui 1992; Daubechies and Bates 1993; Strang and Nguyen 1996; Mallat 1999). Wavelets are scaled and translated versions of a finite-length fast-decaying oscillating waveform called the wavelet function. Wavelet transforms are advantageous over traditional Fourier transforms for representing functions that have discontinuities and sharp peaks, and for accurately deconstructing and reconstructing finite, non-periodic and/or non-stationary signals. The wavelet transform can be expressed as the integral of the scaled and shifted versions of the wavelet function

$$C(\text{scale}, \text{position}) = \int_{-\infty}^{\infty} f(t)\psi(\text{scale}, \text{position}, t)\,dt, \tag{1}$$

where C are the wavelet transform coefficients, f is the function to be transformed and ψ is the wavelet function which depends on the type of wavelet family chosen. The reconstruction of the function f is obtained by the summation of the wavelet coefficients C multiplied by the wavelet function ψ that is scaled and shifted properly. In practice, a sampled version of the continuous wavelet transform described above is used more commonly, which is called the discrete wavelet transform (DWT). In DWT, the signal to be analyzed is fed into high-pass and low-pass filters with certain cut-off frequencies, and the resulting signal is downsampled to obtain an equal number of data as the original signal (see Figure 1).

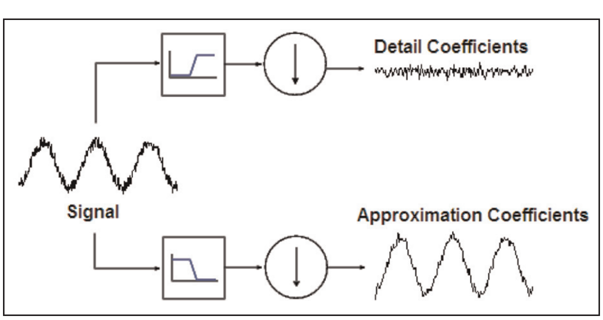

Figure 1. Discrete wavelet transform.

There are numerous families available for wavelet transform, including BNC, Coiflet–Daubechies–Feauveau, Daubechies, Haar, Mathieu, Legendre, Villasenor, and Symlet. It is also possible to apply higher levels of wavelet by applying the wavelet decomposition process over and over to the approximation coefficients. In Figure 2 a multilevel DWT is illustrated.

It is possible to increase the level of the decomposition further; however, the reduction in the number of approximation coefficients will also reduce the resolution so this needs to be kept in mind when choosing an appropriate level.

NS equations

The NS PDEs are among of the most useful sets of equations to describe the behavior of fluid flow. These equations arise from applying Newton's second law to fluid motion, under the assumption that the fluid stress is the sum of a diffusing viscous term plus a pressure term. There are many forms of the NS equations and those to be used for this study are the incompressible NS equations as given in the following:

$$\frac{\partial q}{\partial t} + (q \cdot \nabla)q = -\nabla p + v\Delta q \tag{2}$$

$$\nabla \cdot q = 0 \tag{3}$$

where the second equation is the incompressibility equation. In the above equation, $v \in \mathbb{R}$ is the viscosity value, $p(x, y, t) \in \mathbb{R}$ is the pressure and $q(x, y, t) = (u(x, y, t), v(x, y, t)) \in \mathbb{R}^2$ shows the flow velocity, where u and v are the horizontal and vertical components, respectively. Details of the NS equations can be found in various fluid dynamics texts including Acheson (1990) and Batchelor (2000).

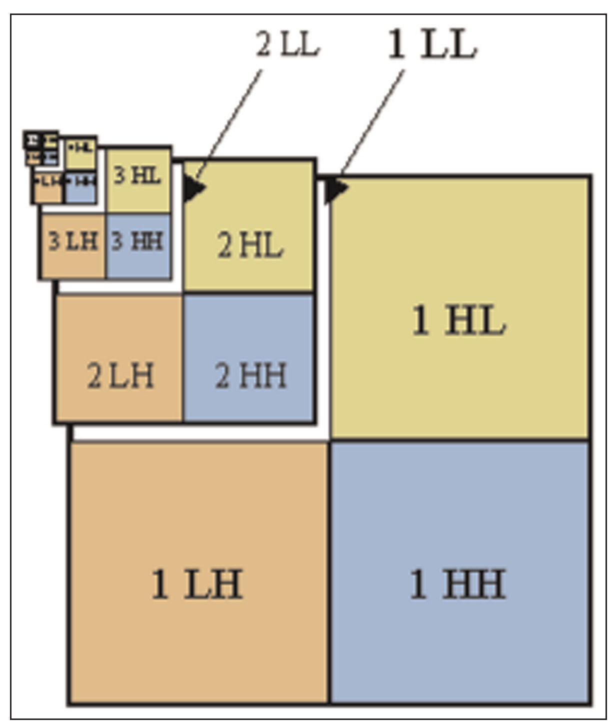

Figure 2. Multilevel two-dimensional wavelet transform.

Modeling and control approach

The first step in the modeling process is to record some snapshots at periodic time intervals using computational fluid dynamics (CFD) simulations of the flow governed by the NS equations (2) and (3). Recall that the goal in the modeling part is to obtain the dynamics is a given region only (as opposed to the entire flow domain). To achieve this effect, we select a set of approximation coefficients whose corresponding wavelet functions tightly cover the area of interest. In addition, we wish to capture the flow behavior at different viscosity values of the fluid. Thus, the CFD simulations are repeated at various viscosity values within a range of interest and the snapshots are recorded for each value. The system input for the simulations is chosen as a chirp signal (i.e. a sinusoid with varying frequency) to excite various modes in the system dynamics. Wavelet decomposition is then applied to these snapshots. As mentioned in the previous section, various options are available as to which wavelet family to choose for the decomposition. Our experience suggests that for snapshots resulting from CFD simulations of flow problems Daubechies wavelet family yields good results. The reason for this is that this wavelet structure is almost random, asymmetric, orthogonal, has finite support area and yields a full reconstruction. In addition, this transformation can be done quite efficiently, which is necessary to process thousands of snapshot images in a reasonable time. As mentioned previously, half of the coefficients obtained from the wavelet decomposition are approximation coefficients and the other half are detail coefficients. To capture the general characteristics of the flow behavior, it is usually sufficient to utilize only the approximation coefficients, but this statement must be verified nevertheless by examining the reconstructions of the flow snapshots from the approximation coefficients. For this purpose the thresholding procedure is applied to the coefficients obtained from wavelet transform. This process can be summarized as follows:

$$Y = \begin{cases} X, & |X| > T, \\ 0, & |X| \leqslant T, \end{cases} \tag{4}$$

where X are detail coefficients, Y are the thresholded coefficients and $T \in \mathbb{R}+$ is the threshold value. The expression shown above states that if the absolute value of a coefficient is greater than the threshold value, this coefficient is saved; otherwise it is set to zero. The reconstruction process is then carried out with the remaining coefficients. As mentioned above, it is desirable that an acceptable reconstruction results even when $T = 0$; this implies that an sufficient reconstruction can be obtained even when only the approximation coefficients are used. This must be confirmed by comparing the approximate reconstructions with the original snapshots, which can be done by simple visual inspection and/or more sophisticated methods such as computing the mean squared error; the former will suffice for the purposes of this paper. Once the approximation coefficients from the wavelet decomposition are at hand, the next step is to construct a system model where these coefficients are the output data, and the input data is the chirp signal used to excite the flow. From this input–output data, a discrete-time state space system as in the following is identified using subspace system identification (N4SID) methods

$$\xi(t + T_s) = A\xi(t) + B\gamma(t), \tag{5}$$

$$y(t) = C\xi(t) + D\gamma(t), \tag{6}$$

where $T_s \in \mathbb{R}$ is sampling time, $\xi \in \mathbb{R}^N$ is the state vector, $n \in \mathbb{N}$ is the degree of the system, $\gamma \in \mathbb{R}$ is the control input and $y \in \mathbb{R}^N$ is the output signal. The output signal consists of the time variation of the approximation coefficients a_i, that is

$$y(t) = a(t) = [a_1(t)\ a_2(t)\ \ldots\ a_N(t)]^{\mathrm{T}}. \tag{7}$$

To briefly summarize, the main point in subspace system identification is the estimation of an extended observability matrix of the form

$$O_r = \begin{bmatrix} C \\ CA \\ \vdots \\ CA^{r-1} \end{bmatrix}. \tag{8}$$

It can be shown that the system output can be expressed in terms of the observability matrix as

$$Y_r(t_k) = O_r\xi(t_k) + S_r\Gamma_r(t_k) + V(t), \tag{9}$$

where

$$Y_r(t_k) = \begin{bmatrix} y(t_k) \\ y(t_{k+1}) \\ \vdots \\ y(t_{k+r-1}) \end{bmatrix}, \Gamma_r(t_k) = \begin{bmatrix} \gamma(t_k) \\ \gamma(t_{k+1}) \\ \vdots \\ \gamma(t_{k+r-1}) \end{bmatrix}, \tag{10}$$

$$S_r = \begin{bmatrix} D & 0 & \cdots & 0 & 0 \\ CB & D & \cdots & 0 & 0 \\ \vdots & \vdots & \ddots & \vdots & \vdots \\ CA^{r-2}B & CA^{r-3}B & \cdots & CB & D \end{bmatrix} \tag{11}$$

and $V(t)$ is the contribution of the output noise. The extended observability matrix is estimated by correlating both sides of (9) with quantities that eliminate the term $S_r\Gamma_r(t_k)$ and $V(t)$ asymptotically. After O_r is estimated, C and A matrices are found by the first row block of O_r and the shifting property. Next, the matrices B, D are estimated using linear least squares utilizing the following alternate representation of (5) and (6)

$$y(t_k) = C(zI - A)^{-1}Bu(t_k) + Du(t_k), \tag{12}$$

where z is the time shift operator. For detailed information about subspace identification methods the reader is referred to Ljung (1999), Van Overschee and De Moor (1996), and Larimore (1996). The subspace identification method is applied to each input–output data set corresponding to individual viscosity values within the desired range, resulting in a discrete-time linear time invariant (LTI) model of the form (5) and (6) for each of these values. The final step in the modeling process is to obtain an uncertain model to capture all of these individual LTI models as a single nominal model plus a multiplicative uncertainty, as illustrated in Figure 3.

In the figure G is the nominal plant, Δ_I is a stable system such that $\|\Delta_I\|_\infty \leqslant 1$ and w_I is a weighting function. The functions Δ_I and w_I form a multiplicative uncertainty on the

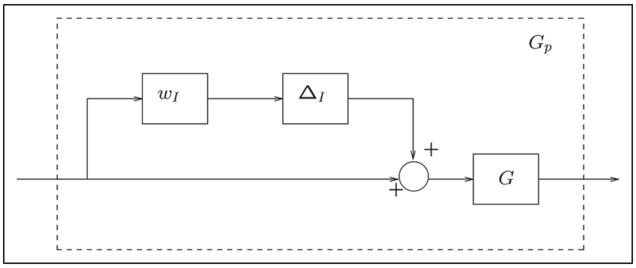

Figure 3. Uncertain system consisting of a nominal model and multiplicative uncertainty.

nominal plant G so that the overall uncertain system G_p is expressed as

$$G_p = G(1 + w_I \Delta_I). \tag{13}$$

The nominal plant G is usually selected so that the effect of the term $w_I \Delta_I$ is small. For the problem of modeling flow conditions under various viscosity values, it generally suffices to pick the plant corresponding to a viscosity value near the center of the desired range. The worst-case deviation of the other models from this nominal model can then be used to fit a multiplicative uncertainty using techniques such as log-Chebyshev magnitude design (Oppenheim and Schaffer 1975). Once this uncertain model is obtained, a robust controller is synthesized via the μ-synthesis D-K iteration method. This method is an approximation to μ-synthesis control design, whose objective is to minimize the structure singular value μ of the robust performance problem related to the uncertain system to be controlled. The uncertain system to be controlled is an open-loop interconnection containing the nominal plant, uncertainty model and possibly weighting filters. Usually the inputs to the system are the disturbances and the output is an error to be minimized (e.g. tracking error). The goal is to construct a stabilizing controller K such that the robust performance μ value is as small as possible. The D-K iteration consists of a series of minimizations. First the D variable associated with the scaled μ upper bound is fixed and a minimization is carried out on the controller variable K. Then, the controller variable K is fixed and a minimization is performed over the D variable. The iteration is repeated as necessary until a controller design is obtained which performs robustly to the modeled uncertainty. The D-K iteration technique may not converge to the minimum μ possible, but the results are satisfactory for the most part. Hence, the D-K iteration approach has enjoyed success in many real-life applications including oscillation suppression in flexible structures, flight control and chemical process control. Details on D-K iteration and its applications can be found in Balas and Doyle (1994), Doyle et al. (1986), Packard et al. (1993), and Stein and Doyle (1991).

In the next section we provide an example to illustrate the modeling and robust control design approach outlined above.

Application example

In this section the modeling and control approaches mentioned in the previous section are illustrated on a sample application. For this purpose we consider the dynamical modeling and control of a fluid flow in the middle of a two-dimensional square region $\Omega = [0,1] \times [0,1] \subset \mathbb{R}^2$, where the fluid viscosity may vary between $[0.000001, 1]$ m^2/s. This viscosity range represents a large number of commonly encountered fluids including acetic acid, ethyl alcohol, crankcase oil, gear oil, benzene, crude oil, fuel oil, gasoline, tar, water and so on. The control goal is to regulate the longitudinal flow velocity at the center of the flow domain. In two dimensions, the NS equations (2) and (3) can be expressed as

$$\frac{\partial u}{\partial t} + \frac{\partial u}{\partial x}u + \frac{\partial u}{\partial y}v = -\frac{\partial p}{\partial x} + \nu\left(\frac{\partial^2 u}{\partial x^2} + \frac{\partial^2 u}{\partial y^2}\right), \tag{14}$$

$$\frac{\partial v}{\partial t} + \frac{\partial v}{\partial x}u + \frac{\partial v}{\partial y}v = -\frac{\partial p}{\partial y} + \nu\left(\frac{\partial^2 v}{\partial x^2} + \frac{\partial^2 v}{\partial y^2}\right), \tag{15}$$

where $q(x,y,t) = (u(x,y,t), v(x,y,t)) \in \mathbb{R}^2$ is the flow velocity with u and v being its horizontal and vertical components, and $p(x,y,t) \in \mathbb{R}$ is the pressure. Initial conditions and boundary conditions for the flow are given as follows:

$$u(x,y,0) = v(x,y,0) = 0, \tag{16}$$

$$u(x,0,t) = u(x,1,t) = 1, \tag{17}$$

$$v(x,0,t) = v(x,1,t) = 0, \tag{18}$$

$$u(0,y,t) = 0, \ \frac{\partial v}{\partial x}(0,y,t) = 0, \tag{19}$$

$$u(1,y,t) = \begin{cases} 0, & y \in [0, 0.42), \\ \gamma(t), & y \in [0.42, 0.58], \\ 0, & y \in (0.58, 1], \end{cases} \tag{20}$$

$$v(1,y,t) = 0, \tag{21}$$

where γ is the control input. The problem described above is an abstract one created specifically to test the effectiveness of the approach proposed in this paper; however, if one desires to attribute a physical meaning, it is possible to think of the flow domain as a cavity with the top and bottom walls being driven at constant speed, the left wall being a membrane or filter allowing the fluid to pass horizontally, and the right wall being stationary with a small slit of width 0.16 positioned at its center through which fluid can be pumped or sucked. The first step in the modeling process is to simulate the NS equations under a varying frequency sinusoid (chirp signal) and under different viscosity values in the range $[0.000001, 1]$. For this purpose Navier2D, a NS CFD solver for MATLAB (Engwirda 2005), is used and the snapshots are recorded for 1000 time steps on a 50×50 uniform grid of the spatial domain. Wavelet decomposition is then performed on these snapshots using functions from the MATLAB Wavelet Toolbox. We have experimented with many wavelet families and decomposition levels and the best results (i.e. the least error in reconstruction) were obtaining using the Daubechies-4 wavelet and a two-level decomposition. To verify that this wavelet function and level is adequate for the method considered, a flow snapshot together with its wavelet decomposition and its reconstruction using only the approximation coefficients (i.e. after thresholding the detail coefficients to zero) are shown in Figure 4.

It can be seen from the figure that the original snapshot and its reconstruction are almost identical. Such a comparison was performed with other snapshots as well and the results were equally satisfactory. The next step is to select a number of approximation coefficients whose corresponding basis functions cover the area of interest. Since we are interested in the center region only, for our case it suffices to select the four basis functions that are closest to the center of the domain, as shown in Figure 5.

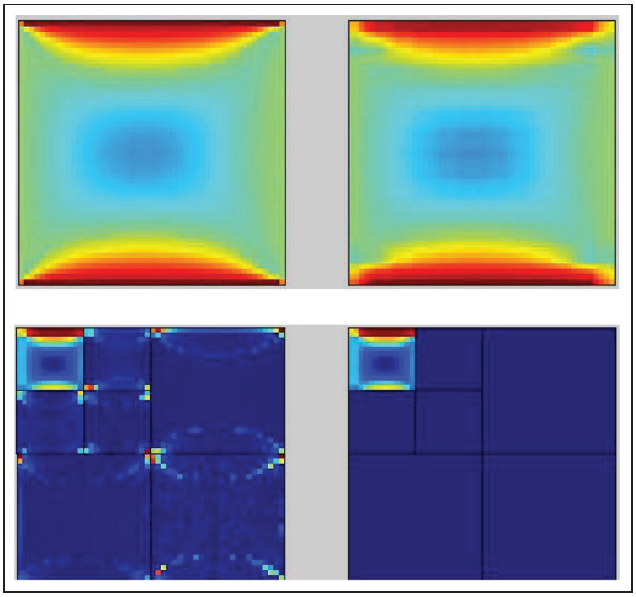

Figure 4. Original snapshot (top left), wavelet coefficients resulting from two-level decomposition using Daubechies-4 wavelet (bottom left), thresholded wavelet coefficients (bottom right) and snapshot reconstructed from thresholded coefficients (top right).

The next process is to fit a linear state-space model for each viscosity value to the time dynamics of these four approximation coefficients. We select 10 viscosity values in the range [0.000001, 1] to build these models. The 10 particular viscosities selected are $v_1 = 0.00000100$, $v_2 = 0.00001931$, $v_3 = 0.00037276$, $v_4 = 0.00719686$, $v_5 = 0.07142950$, $v_6 = 0.21428650$, $v_7 = 0.37275937$, $v_8 = 0.57142900$, $v_9 = 0.78571450$ and $v_{10} = 1.00000000$, which are approximately logarithmically spaced so that more values are concentrated towards the lower limit 0.000001. This is beneficial for the modeling process since the flow dynamics show greater variation for lower viscosities due to turbulent characteristics and therefore more samples are needed from these values for an accurate model. Selecting more than 10 values for v could also improve the model; however, this will not be necessary for the particular problem at hand as it will be observed shortly that the model resulting from the values above is satisfactory.

As mentioned in the previous section, a subspace system identification (N4SID) is carried out to obtain these model by the help of functions from the MATLAB System Identification Toolbox. Based on the input output data and the Hankel singular values of the resulting models (see Glover 1984), it can be shown that a system order of 6 is

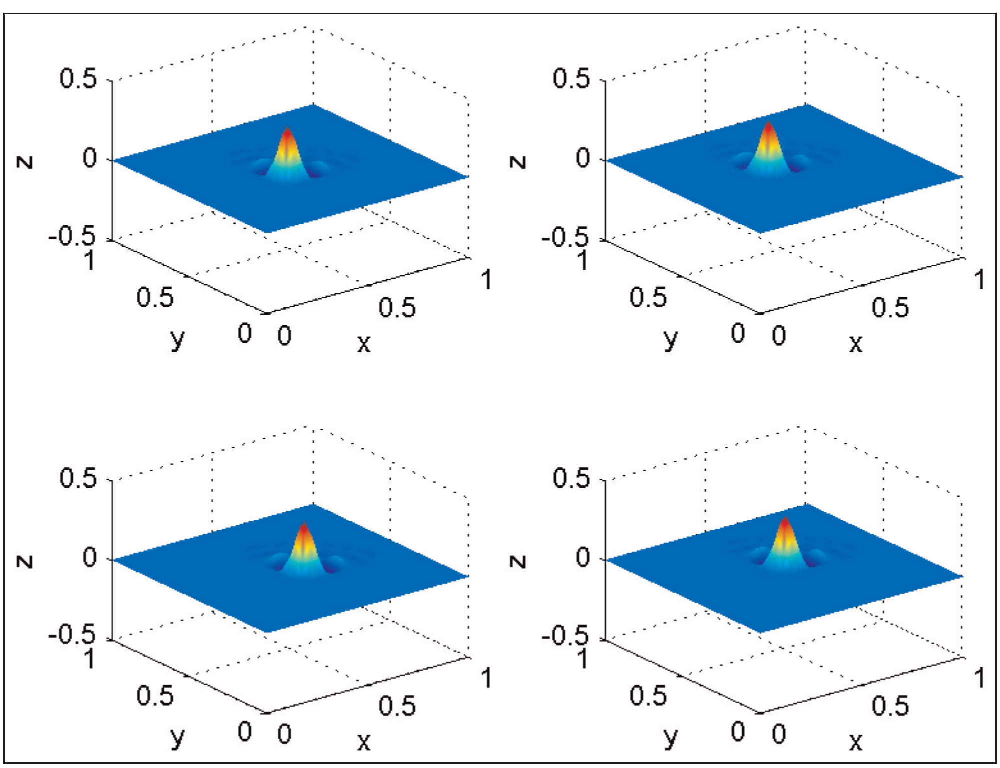

Figure 5. Four approximation coefficients for describing the middle of the flow region.

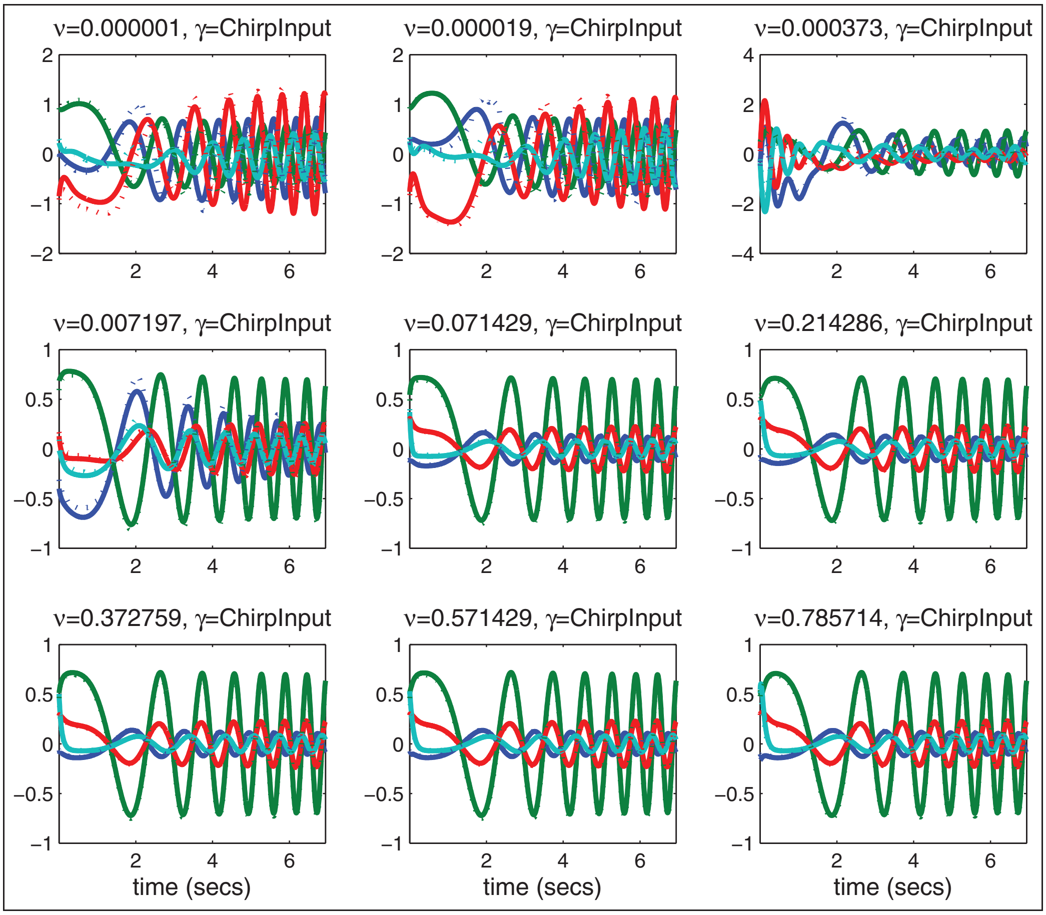

Figure 6. Approximation coefficients (solid) versus the results outputs of the models fit to data (dashed) for different viscosity values.

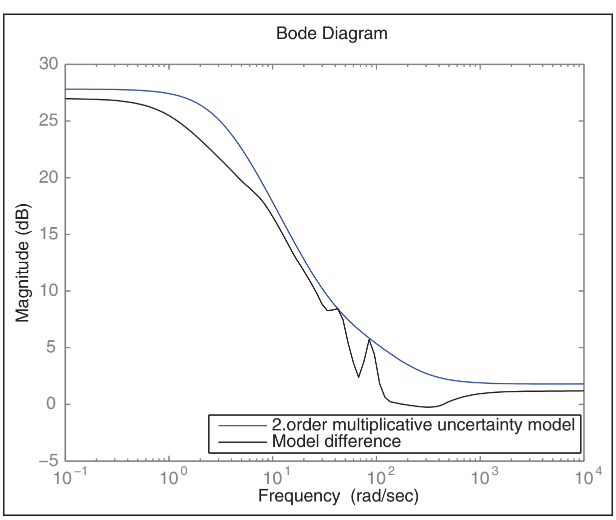

Figure 7. Bode magnitude plot of the second-order multiplicative uncertainty model and the difference between nominal model and the models at various viscosities.

sufficient for the models. Figure 6 shows the outputs of these models built in comparison with the actual time variation of the four approximation coefficients selected to represent the central region. It can be seen that there is good agreement between the actual values and those produced by the models. The error is almost zero for higher viscosity values and increases slightly with the decrease in viscosity. This is expected since at lower viscosity values the turbulent characteristics of the flow become more dominant, hence the dynamics become more difficult to capture.

Next, these 10 models are combined into a single uncertain model which consists of a second-order multiplicative uncertainty model and a nominal model, which is simply the model built for $v_7 = 0.37275937$. The reason for selecting this viscosity value is that it yields the smallest magnitude for the uncertainty model. Figure 7 shows a Bode plot comparing the norm of the difference between the nominal model and the array of models at different viscosity values versus the magnitude of the second-order multiplicative weight.

It is seen that the range of behavior of the multiplicative uncertainty includes the array of systems at different viscosities for the entire frequency range. The next step is to a build a robust controller to achieve the desired tracking for this uncertain system via D-K iteration algorithm. The controller synthesis is carried out using the dksyn command of the MATLAB Robust Control Toolbox, which results in a 12th-order controller, which is of quite high order for efficient incorporation into CFD simulations. However, examining the

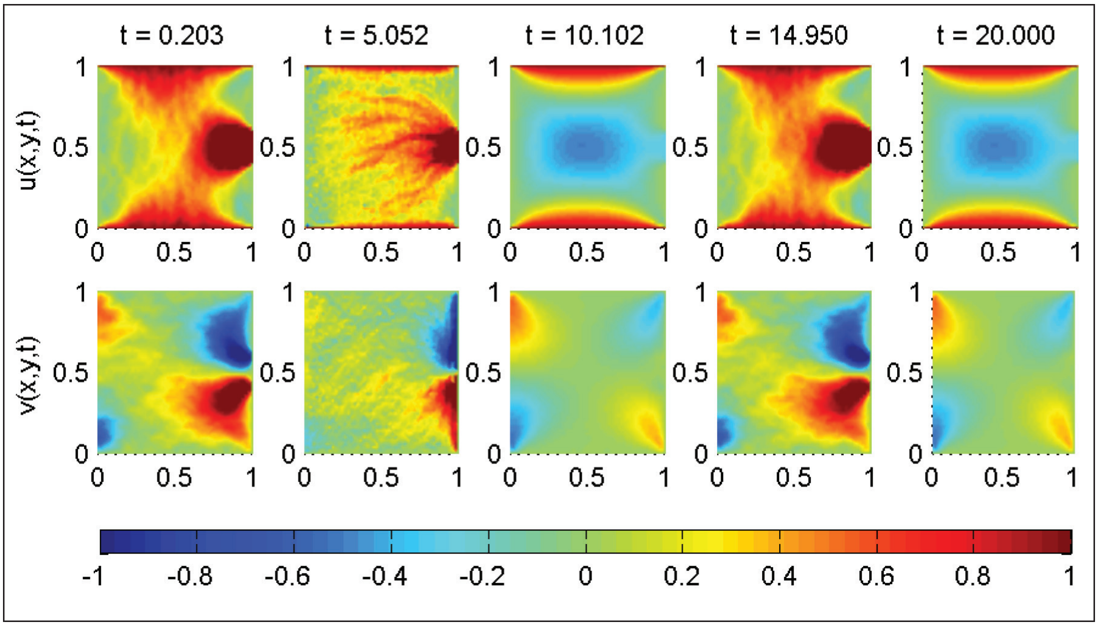

Figure 8. Flow snapshots from CFD simulations of the closed-loop system with D-K iteration based controller.

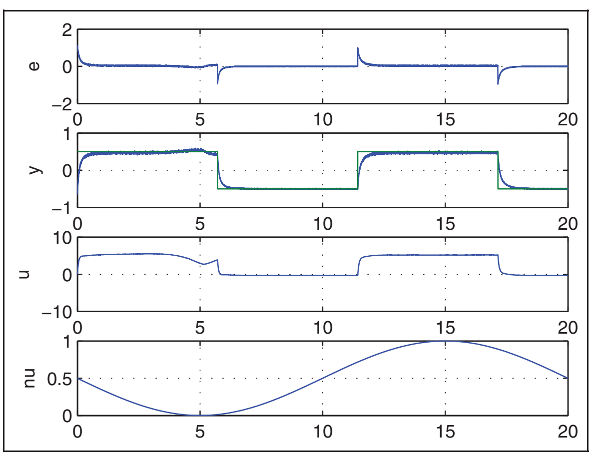

Figure 9. Time variations of key signals for D-K iteration based control. First figure (from top): Tracking error. Second: Longitudinal speed at the center (blue) and reference signal (green). Third: Control input. Fourth: Viscosity variation. Color refers to the online version of this article.

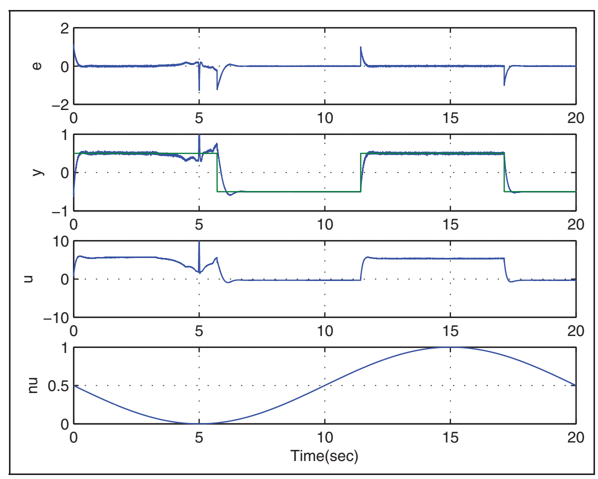

Figure 10. Time variations of key signals for PID-based control. First figure (from top): Tracking error. Second: Longitudinal speed at the center (blue) and reference signal (green). Third: Control input. Fourth: Viscosity variation. Color refers to the online version of this article.

Hankel singular values it is seen the controller can effectively be approximated by a third-order system, which is acceptable. The transfer function for this controller is as follows:

$$K(z) = \frac{0.1334z^2 - 0.2658z + 0.1324}{z^3 - 2.98z^2 + 2.96z - 0.98}. \tag{22}$$

The final step is to perform CFD simulations in closed-loop with the controller (22) above. In the simulations the viscosity value ν is varied between its limits 0.000001 and 1, while the reference y_{ref} to be tracked by the midpoint of the domain is varied between -0.5 and 0.5. White noise disturbances of magnitude 0.05 have also been added to the system input and output. Figure 8 shows the flow snapshots obtained from the simulations and Figure 9 shows the output value at the center point, the tracking error, the control input, and the variation in ν. It can be seen that the reference is tracked closely despite the variations in viscosity. Slight deviations are observed around the region where the viscosity is near its lower limit (around $t = 5$ seconds), which is expected since these intervals correspond to the situation where the flow characteristics are more turbulent.

For the sake of comparison with the D-K iteration based robust controller, we have designed a simple PID controller using only the nominal model for the system and have repeated the CFD simulations for this case. Various automated tuning algorithms were considered to design the PID controller and the best results that could be obtained were with the IMC tuning based approach (Chien and Fruehauf 1990). The closed-loop simulation results for this case are shown in Figure 10.

It can be seen from the figure that the controller performance is acceptable for the relatively less problematic situations of high viscosity. However, for the case when the viscosity is low (around $t = 5$ seconds) and thus the flow characteristics are turbulent, there is a considerable deviation from the reference to be tracked and the tracking performance is clearly inferior to the D-K-based controller case (Figure 9).

Conclusions and future work

In this paper a new approach for the modeling and control of flow problems has been introduced to achieve local dynamical modeling and control when the fluid viscosity is unmeasurable and non-constant. The modeling relies on wavelet transform of the flow snapshots obtained from CFD simulations. The control synthesis relies on applying the D-K iteration synthesis method to an uncertain model built by encapsulating separate models at each viscosity value. This results in a robust controller that can control the system for the desired range of viscosities without requiring online viscosity measurements. The approach has been illustrated on a sample flow problem where the goal is to regulate the longitudinal speed at the center of the flow domain. It is seen through CFD simulations that the closed-loop systems successfully tracks a given reference even when the fluid viscosity is varying continually. The results have been compared with a PID-based controller based on a nominal model and it is seen that the robust controller based on D-K iteration is superior to the PID controller, especially at lower values of the viscosity where the flow characteristics become more turbulent.

Future research directions include incorporating alternative robust control synthesis approaches and testing the ideas on more complicated flow control problems.

Acknowledgement

We are grateful to the libraries of TOBB University of Economics and Technology for providing valuable resources used in this study.

Funding

This work was supported by The Scientific and Technological Research Council of Turkey (TÜBİTAK) through project number 109E233.

References

Acheson DJ (1990) *Elementary Fluid Dynamics*. Oxford: Oxford University Press.

Balas GJ and Doyle JC (1994) Robust control of flexible modes in the controller crossover region. *AIAA Journal of Guidance, Dynamics and Control* 12: 370–377.

Batchelor GK (2000) *An Introduction to Fluid Dynamics*. Cambridge: Cambridge University Press.

Bewley TR (2001) Flow control: new challenges for a new Renaissance. *Progress in Aerospace Sciences* 37: 21–58.

Camphouse RC (2005) Boundary feedback control using Proper Orthogonal Decomposition models. *Journal of Guidance, Control, and Dynamics* 28: 931–938.

Chien IL and Fruehauf PS (1990) Consider IMC tuning to improve controller performance. *Chem Eng Prog* 86(10): 33–41.

Chui CK (1992) *An Introduction to Wavelets*. New York: Academic Press.

Daubechies I and Bates B (1993) Ten Lectures on Wavelets. *The Journal of the Acoustical Society of America* 93: 1671.

Doyle J, Lenz K and Packard A (1986) Design examples using μ-synthesis: space shuttle lateral axis FCS during reentry. In *25th IEEE Conference on Decision and Control*.

Efe MO and Ozbay H (2004) Low dimensional modelling and Dirichlet boundary controller design for Burgers equation. *International Journal of Control* 77: 895–906.

Engwirda D (2005) *An Unstructured Mesh Navier–Stokes Solver*. Master's thesis, School of Engineering, University of Sydney.

Gad-el Hak M (2000) *Flow Control—Passive, Active, and Reactive Flow Management*. New York: Cambridge University Press.

Glover K (1984) All optimal Hankel-norm approximations of linear multivariable systems and their L-infinity error bounds. *International Journal of Control* 39: 1115–1193.

Holmes P, Lumley J and Berkooz G (1996) *Turbulence, Coherent Structures, Dynamical System, and Symmetry*. Cambridge: Cambridge University Press.

Kasnakoglu C, Serrani A and Efe MO (2008) Control input separation by actuation mode expansion for flow control problems. *International Journal of Control* 81: 1475–1492.

Larimore WE (1996) Statistical optimality and canonical variate analysis system identification. *Signal Processing* 52: 131–144.

Ljung L (1999) *System Identification: Theory for the User*. Upper Saddle River, NJ: Prentice Hall.

Mallat S (1999) *A Wavelet Tour of Signal Processing*. New York: Academic Press.

Oppenheim A and Schaffer R (1975) *Digital Signal Processing*. Englewood Cliffs, NJ: Prentice Hall.

Packard A, Doyle J and Balas G (1993) Linear, multivariable robust control with a μ perspective. *Journal of Dynamic Systems, Measurement, and Control* 115: 426.

Sirovich L (1987) Turbulence and the dynamics of coherent structures. *Q Appl Math* 45: 561–590.

Stein G and Doyle J (1991) Beyond singular values and loop shapes. *AIAA Journal of Guidance and Control* 14: 5–16.

Strang G and Nguyen T (1996) *Wavelets and Filter Banks*. Wellesley, MA: Cambridge University Press.

Van Overschee P and De Moor B (1996) *Subspace Identification for Linear Systems: Theory, Implementation, Applications*. Dordrecht: Kluwer Academic Publishers.